signal and frequency conversion have been discussed also. Here, intuitively expected results are studied by the symmetrical formulation proposed.

The success of the symmetrical formalism depends on the feasibility of evaluating (3) and (4) by means of x ordering; it is intuitively plausible. The arguments presented, although lacking mathematical rigor, have demonstrated and justified the validity of this procedure in dealing with traveling waves propagating along a unique forward direction. It is interesting to note that not only the parametric interactions considered here deal with waves traveling forward in a unique dimension, but most experiments in coherent nonlinear optics are in this situation.

ACKNOWLEDGMENTS

The author wishes to thank Professor R. A. Phillips for his comments on the manuscript, and to thank Professor W. B. Cheston and T. A. Holl for their interest in this work.

PHYSICAL REVIEW VOLUME 176, NUMBER 2 10 DECEMBER 1968

Spin–Lattice Coupling Constants of an Fe^{3+} Ion in MgO

R. R. Sharma
Department of Physics, University of Illinois, Chicago, Illinois
(Received 27 May 1968)

Estimates of the spin-lattice coupling constants of an Fe^{3+} ion in the host crystal MgO have been made. There are only two independent coupling constants C_{11} and C_{44} in the simple case of a cubic lattice. Various possible mechanisms contributing to the coupling constants in the point-charge model have been investigated. It has been shown that the Blume-Orbach mechanism is the dominant one among the mechanisms considered. The next most important contribution arises from the spin-spin interaction mechanism proposed by Pryce. The other mechanisms which we have considered are found to give an entirely negligible contribution to the coupling constants. The combined point-charge contributions arising from all the mechanisms are, in units of 10^{-13} cm/dyn, C_{11}(point-charge) $=+2.11$ and C_{44}(point-charge) $=-3.06$, as compared with the experimental results, in the same units, C_{11}(expt) $=+26$ and C_{44}(expt) $=-5.5$, due to Feher. Also, the estimated overlap contributions to C_{11} and C_{44} are found to be an order of magnitude less than the point-charge contributions. Finally, some suggestions have been made in order to bring the theoretical results into better agreement with the experimental results.

I. INTRODUCTION

It has been shown earlier[1,2] that the zero-field splitting parameters D and E occurring in the spin Hamiltonian

$$H_S = D[3S_z^2 - S(S+1)] + E(S_x^2 - S_y^2) \qquad (1)$$

can be explained reasonably well in the case of Mn^{2+} contained in ZnF_2 and MnF_2. The effects of the crystal fields at the site of the paramagnetic ion Mn^{2+} in the host lattice and the overlap due to the ligand ion wave functions were taken into account. It was concluded[1] that the dominant contribution arose from the Blume-Orbach[3] (BO) mechanism, which involves the first-order matrix element of the axial and rhombic fields, and second-order matrix elements of the spin-orbit interaction between excited quartet states which have been admixed into one another by the presence of the cubic field. The next most important mechanism was shown to be the spin-spin mechanism[4] (Pryce mechanism), linear in both spin-spin interaction and axial or rhombic crystal fields. The Orbach-Das-Sharma mechanism[4] (ODS) and the Watanabe mechanism[1,5] in the presence of cubic field (WC) follow the spin-spin mechanism in decreasing order of importance. The overlap contributions were also investigated[2] and found to be important.

The agreement between the theory and the experimental results for Mn^{2+} has prompted the analysis of the various mechanisms for Fe^{3+} present in different crystal symmetries. In this paper, the example of Fe^{3+} situated in the host crystal MgO distorted by an uniaxial stress is considered. The undistorted MgO crystal has a cubic lattice, and therefore by symmetry both D and E parameters vanish. However, one can create a noncubic environment about the paramagnetic-ion (Fe^{3+}) site by applying uniaxial stress, and therefore obtain nonvanishing parameters D and E. When the parameters D and E are expressed as linear functions of the applied stress, there are only two independent constants[6] of proportionality in the simple case of a cubic crystal. These are spin-lattice constants C_{11} and C_{44}. Experimental results are available for these con-

[1] R. R. Sharma, T. P. Das, and R. Orbach, Phys. Rev. **149**, 257 (1966), hereafter referred to as I.
[2] R. R. Sharma, T. P. Das, and R. Orbach, Phys. Rev. **155**, 338 (1967), hereafter referred to as II.
[3] M. Blume and R. Orbach, Phys. Rev. **127**, 1587 (1962).
[4] M. H. L. Pryce, Phys. Rev. **80**, 1107 (1950); A. S. Chakravarty, J. Chem. Phys. **39**, 1004 (1963); R. Orbach, T. P. Das, and R. R. Sharma, in *Proceedings of the International Conference on Magnetism, Nottingham, 1964* (The Institute of Physics and the Physical Society, London, 1965), p. 330.
[5] H. Watanabe, Progr. Theoret. Phys. (Kyoto) **18**, 405 (1957).
[6] G. D. Watkins and E. Feher, Bull. Am. Phys. Soc. **7**, 29 (1962); N. S. Shiren, *ibid.* **7**, 29 (1962); E. Feher, Phys. Rev. **136**, A145 (1964).

stants in the case of MgO:Fe^{3+} under stress from the studies of Watkins and Feher, Shiren, and Feher.[6] Stresses along the [001] direction in order to compute C_{11} and along the [110] direction to compute C_{44} may be considered. For these two cases the rleations between C_{11} and C_{44} and the parameters D and E appearing in Eq. (1) are given by Feher.[6] When the stress X' is applied along the [001] direction, the relations are

$$D=\tfrac{1}{2}C_{11}X',$$
$$E=0;$$

and for the stress X' along the [110] direction, these are

$$D=-\tfrac{1}{4}C_{11}X',$$
$$E=\tfrac{1}{2}C_{44}X'.$$

Thus the parameters D and E for a known stress X' can be used to obtain the spin-lattice constants C_{11} and C_{44}.

As mentioned above, the first case (X' along [001] direction) may be used to determine D (or C_{11}) and the second case (X' along [110] direction) to determine E (or C_{44}). Both the point-multipole and overlap models are taken into account. The various mechanisms (BO, spin-spin, ODS, and WC) which contribute to D and E are analyzed. For purposes of calculation it is assumed that the elastic constants around Fe^{3+} are the same as for the pure MgO lattice, and that the distortion around the Fe^{3+} ion due to the applied stress is the same as in pure MgO under the same stress.

In the following section, the point-multipole contributions to D and E are analyzed for MgO:Fe^{3+} under stress. The overlap contributions are considered in Sec. III. The last section is devoted to the discussion of our results, and some suggestions are made in order to improve the theoretical situation.

II. POINT-CHARGE CONTRIBUTIONS TO D AND E

General expressions for D and E for Blume-Orbach (BO), spin-spin (Pryce), ODS, and Watanabe with cubic field (WC) mechanisms in the presence of axial and rhombic crystal fields have already been derived.[1] However, for the sake of convenience, they are listed in Appendix A. Since, from calculations, it is found that the contributions D_{ODS} and D_{WC} are negligible, similar contributions to E should also be negligible. Hence, the expressions for E_{ODS} and E_{WC} are not presented in the Appendix here.

The evaluation of the contributions from the BO, ODS, and WC mechanisms [as evident from the expressions (A1), (A2), (A13), and (A16)] requires the knowledge of the coefficients α_i, β_i, γ_i, and the eigenvalues Δ_i. These are determined by diagonalizing the $^4\Gamma_4$ matrix in the presence of the cubic field.[1] For Fe^{3+}, taking the energy values[7] $E(^4G)=0.320\times10^5$, $E(^4P)=0.351\times10^5$, and $E(^4F)=0.521\times10^5$, in units of cm^{-1} relative to the ^6S level, the values of α_i, β_i, γ_i, and Δ_i for $10Dq=16\,000$, 17 000, and 18 000 cm^{-1} are listed in Table I.

Using Table I, the parameters $p_{\alpha\alpha}$, $p_{\alpha\beta}$, and $p_{\alpha\gamma}$ defined in (A5) can now be calculated. The calculated values for $10Dq=18\,000$ cm^{-1} are found to be

$$p_{\alpha\alpha}=3.749\times10^{-5}\ \mathrm{cm},$$
$$p_{\alpha\beta}=-0.303\times10^{-5}\ \mathrm{cm},$$
$$p_{\alpha\gamma}=1.963\times10^{-5}\ \mathrm{cm}. \qquad (2)$$

The expressions from spin-spin and ODS mechanisms [Eqs. (A6)–(A9), (A11), (A13), and (A14)] involve the integrals $g_{d\to l}^{n,n+3}$, $h_{d\to l}^{n,n+3}$, and $\langle u_d^0 \mid r^2 \mid u_{d\to l}^{(1)}\rangle$, and these require the perturbation functions $u_{d\to s}^{(1)}$, $u_{d\to d}^{(1)}$, and $u_{d\to g}^{(1)}$. These functions are obtained by employing Numerov's method[8] and Watson's Hartree-Fock solution[9] u_d^0 of the $3d$ wave function for Fe^{3+} and integrating the differential equations (A12) numerically. The numerical solutions for $u_{d\to s}^{(1)}$, $u_{d\to d}^{(1)}$, and $u_{d\to g}^{(1)}$ so obtained are plotted in Fig. 1. The values of $g_{d\to l}^{n,n+3}$ and $h_{d\to l}^{n,n+3}$ for required values of n and l are, then, calculated and listed in Table II. The values obtained for other integrals $\langle u_d^0 \mid r^2 \mid u_{d\to l}^{(1)}\rangle$, are in atomic units,

$$\langle u_d^0 \mid r^2 \mid u_{d\to s}^{(1)}\rangle=1.5557,$$
$$\langle u_d^0 \mid r^2 \mid u_{d\to d}^{(1)}\rangle=0.4960,$$
$$\langle u_d^0 \mid r^2 \mid u_{d\to g}^{(1)}\rangle=0.4520. \qquad (3)$$

TABLE I. The values of α_i, β_i, γ_i, and Δ_i for the Fe^{3+} ion.

i	α_i	β_i	γ_i	Δ_i (cm^{-1}) measured from ^6S
		$10Dq=16\,000$ cm^{-1}		
1	0.706	0.506	−0.494	45 116
2	0.640	−0.159	0.752	18 297
3	0.302	−0.847	−0.437	55 787
		$10Dq=17\,000$ cm^{-1}		
1	0.692	0.545	−0.473	45 494
2	0.641	−0.164	0.750	17 328
3	0.331	−0.822	−0.463	56 378
		$10Dq=18\,000$ cm^{-1}		
1	0.678	0.580	−0.452	45 828
2	0.642	−0.168	0.748	16 358
3	0.358	−0.797	−0.487	57 014

[7] Charlotte E. Moore, Natl. Bur. Std. (U.S.) Circ. **467** (1949).

[8] D. R. Hartree, *The Calculation of Atomic Structure* (John Wiley & Sons, Inc., New York, 1957), p. 71.

[9] R. E. Watson, Massachusetts Institute of Technology Technical Report No. 12, SSMT Group (unpublished).

TABLE II. The quantities $g_{d\to l}^{n,n+3}$ and $h_{d\to l}^{n,n+3}$. Integrals not required are not given.

n	$g_{d\to s}^{n,n+3}$	$h_{d\to s}^{n,n+3}$	$g_{d\to d}^{n,n+3}$	$h_{d\to d}^{n,n+3}$	$g_{d\to g}^{n,n+3}$	$h_{d\to g}^{n,n+3}$
0	...	−0.18537	−0.15985	−0.09987	...	0.04236
2	−0.13035	...	−0.08457	−0.06499	0.00912	0.01824
4	...	...	...	...	...	0.01093

The various contributions to D and E (in units of cm^{-1}) for Fe^{3+} in terms of the crystal-field components can be written as follows:

$$\begin{aligned}
&D_{BO}=4.6578(B_4^0)', && E_{BO}=-17.6746B_4^2,\\
&D_{SS}(d\to s)=-0.0131B_2^0, && E_{SS}(d\to s)=-0.0119B_2^2,\\
&D_{SS}(d\to d)=-0.1261B_2^0, && E_{SS}(d\to d)=-0.00694B_2^2,\\
&D_{SS}(d\to g)=-0.0213B_2^0, && E_{SS}(d\to g)=-0.0258B_2^2,\\
&D_{SS}(\text{total})=-0.1605B_2^0, && E_{SS}(\text{total})=-0.0446B_2^2.\\
&D_{ODS}=0.5312(B_2^0)^2,\\
&D_{WC}=-1.2090(B_2^0)^2.
\end{aligned} \tag{4}$$

In deriving the above expressions, the following values were used: $\zeta=400$ cm^{-1}, $\Delta_{DS}=3.85\times10^4$ cm^{-1} for the energy[7] of the ^4D level relative to the ^6S state; the values (2) for the parameters $p_{\alpha\alpha}$, $p_{\alpha\beta}$, $p_{\alpha\gamma}$, the integrals $g_{d\to l}^{n,n+3}$ and $h_{d\to l}^{n,n,+3}$ from Table II, and the calculated values of $\langle r^2\rangle=1.1500$ and $\langle r^4\rangle=2.7894$ in atomic units. The crystal fields $(B_4^0)'$ and (B_4^2) in (4) are in units of $e^2/2a_0^5$, and B_2^0 and B_2^2 are in units of $e^2/2a_0^3$, a_0 being the Bohr radius.

When the stress is applied along [001] direction of the crystal, E is zero by symmetry and D can be determined from (4) if one knows $(B_4^0)'$ and B_2^0. In evaluating $(B_4^0)'$ and B_2^0 we assume that the elastic constants around the paramagnetic impurity ion are the same as in the pure host lattice, and that the distortion around it due to the applied stress is the same as in the pure lattice. In other words, the lattice relaxation due to the presence of the impurity ion has not been taken into account.

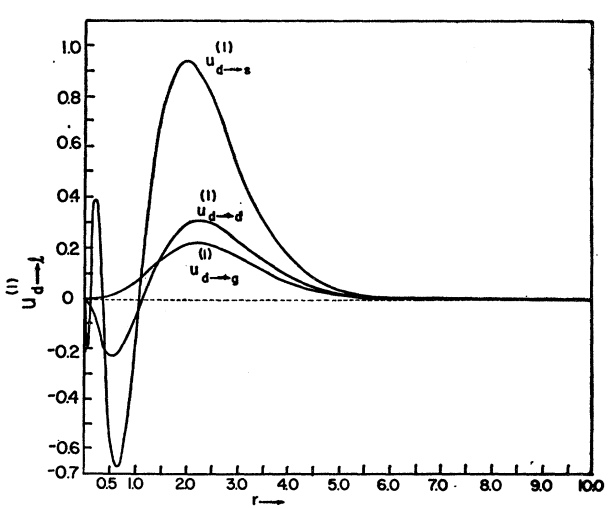

FIG. 1. Plot of $u_{d\to s}^{(1)}$, $u_{d\to d}^{(1)}$, and $u_{d\to g}^{(1)}$ for Fe^{3+}. All quantities are in atomic units.

For stress along the [001] direction, the strain components e_{xx}, e_{yy}, and e_{zz} are given by

$$e_{xx}=e_{yy}=-\frac{c_{12}X'}{(c_{11}-c_{12})(c_{11}+2c_{12})},$$

$$e_{zz}=\frac{(c_{11}+c_{12})X'}{(c_{11}-c_{12})(c_{11}+2c_{12})}, \tag{5}$$

where c_{11} and c_{12} are the two elastic constants for a cubic crystal. For MgO lattice these are[10]

$$c_{11}=29.54\times10^{11}\ \text{dyn/cm}^2,$$
$$c_{12}=8.49\times10^{11}\ \text{dyn/cm}^2. \tag{6}$$

It can be seen with the help of (5) and (6) that in MgO, the stress $X'=600$ kg/cm^2 $=0.5886\times10^9$ dyn/cm^2 along [001] gives rise to the strain components

$$e_{xx}=e_{yy}=-0.5103\times10^{-4}$$

and

$$e_{zz}=2.2859\times10^{-4}. \tag{7}$$

The change in the dimensions of a unit cubic cell is given by

$$\Delta x=\Delta y=ae_{xx}=ae_{yy},$$
$$\Delta z=ae_{zz}, \tag{8}$$

where a is the dimension of original cubic cell, which in the case of MgO is 4.203 Å. Thus, the new cell dimen-

[10] A. L. Schawlow, A. H. Piksis, and S. Sugano, Phys. Rev. 122, 1469 (1961).

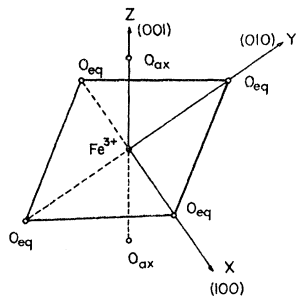

FIG. 2. Positions of the nearest-neighbor O^{2-} ions around Fe^{3+} ion for stress along [001] direction, and the disposition of the crystal axes X, Y, and Z.

sions, if denoted by a', b', and c', become

$$a'=a(1+e_{xx})=b',$$
$$c'=a(1+e_{zz}). \tag{9}$$

The crystal-field components can now be calculated for this distorted lattice. The explicit expressions for (B_2^0) and $(B_4^0)'$ in units of $e^2/2a_0^3$ and $e^2/2a_0^5$, respectively, are given by[1]

$$B_2^0=\sum_j q_j(3\cos^2\Theta_j-1)/R_j^3,$$
$$(B_4^0)'=(B_4^0)_{\rm nc}-\alpha(B_4^4)_{\rm nc}, \tag{10}$$

with

$$(B_4^0)_{\rm nc}=\tfrac{1}{4}\sum_j q_j(35\cos^4\Theta_j-30\cos^2\Theta_j+3)/R_j^5,$$
$$(B_4^4)_{\rm nc}=\tfrac{1}{8}(70)^{1/2}\sum_j q_j[\sin^4\Theta_j\cos(4\Phi_j)]/R_j^5,$$
$$\alpha=(B_4^0)_{\rm c}/(B_4^4)_{\rm c},$$
$$(B_4^0)_{\rm c}=\tfrac{1}{4}\sum_j^{\rm c} q_j(35\cos^4\Theta_j-30\cos^2\Theta_j+3)/R_j^5,$$
$$(B_4^4)_{\rm c}=\tfrac{1}{8}(70)^{1/2}\sum_j^{\rm c} q_j[\sin^4\Theta_j\cos(4\Phi_j)]/R_j^5, \tag{11}$$

where R_j is in units of a_0, c stands for the cubic lattice, and nc for the distorted (noncubic) lattice; and the summation runs over all the external ions (constituting the lattice) with charge $q_j\,|\,e\,|$ situated at (R_j, Θ_j, Φ_j) with respect to an origin at the site of the paramagnetic ion.

Recently, there has been some confusion (in applying[11] the theory[1] to the zero-field splitting of $Cd_2V_2O_7$:Mn^{+2}) as regards the sign of the quantity α and the accurate determination of $(B_4^0)'$. Therefore, it is worthwhile to give some details concerning the computation of α and $(B_4^0)'$. Considering Fig. 2, which shows the nearest neighbors disposed around the paramagnetic ion, if the X and Y axes are rotated by $\pi/4$ about Z axis, it can be seen that the quantity α changes sign since $(B_4^4)_{\rm c}$ changes sign, whereas $(B_4^0)_{\rm c}$ does not. Also, under the same rotation, the component $(B_4^0)_{\rm nc}$ does not change sign, while $(B_4^4)_{\rm nc}$ does change sign. Consequently, $(B_4^0)'$, as defined in (10), remains unchanged in magnitude and sign under this rotation. So, even though the quantity α changes sign, the quantity $(B_4^0)'$ remains unaltered. Therefore, it is essential that all crystal-field components be evaluated with respect to the same axis system. Otherwise, instead of the subtractive unbalanced noncubic part $(B_4^0)'$, an additive result of the components $(B_4^0)_{\rm nc}$ and $\alpha(B_4^4)_{\rm nc}$ would be obtained, and this is a large part.

In order to compute the crystal fields, a direct lattice summation method can be adopted. In this method, the crystal is divided into different spherical shells about the impurity ion with the radii na', where $n=1, 2, 3, \cdots$, etc., and a' is given by (9). Next a neutral group consisting of four atoms of Mg^{2+} and four atoms of O^{2-} is formed in each crystal cell. The neutral group is assumed to contribute to a shell in which the center of the group lies. Then, starting from the smallest shell, the contributions to various B_l^m from bigger shells are summed one by one until the contribution of the next shell becomes negligibly small. This method is found to be very useful for computing B_2^0, which is otherwise not very convergent. The calculated values are

$$(B_4^0)'=(B_4^0)_{\rm nc}-(14/5)^{1/2}(B_4^4)_{\rm nc}$$
$$=(0.1501\times10^{-4})\ e^2/2a_0^5,$$
$$B_2^0=(0.5299\times10^{-4})\ e^2/2a_0^3. \tag{12}$$

The values in Eq. (12) were also checked with the help of the Nijboer and de Wette's method[12] to ensure the accuracy of the calculated crystal fields.

The induced quadrupole and higher multipole moments can give an additional contribution to these crystal-field components. Since these are not currently available, only the point-charge estimates (12) have been used to compute $D_{\rm BO}$, $D_{\rm SS}$, $D_{\rm ODS}$, and $D_{\rm WC}$ from the expressions (4). The calculated results (in units of 10^{-4} cm^{-1}) are

$$D_{\rm BO}=0.70,$$
$$D_{\rm SS}(d\to s)=-0.0069,$$
$$D_{\rm SS}(d\to d)=-0.0668,$$
$$D_{\rm SS}(d\to g)=-0.0113,$$
$$D_{\rm SS}({\rm total})=-0.0850,$$
$$D_{\rm ODS}=+0.000016,$$
$$D_{\rm WC}=-0.000034. \tag{13}$$

Summing these, we get the total point-charge contribution to D as

$$D({\rm point\text{-}charge})=+0.62\times10^{-4}\ {\rm cm}^{-1}. \tag{14}$$

[11] C. V. Stager, Can. J. Phys. **46**, 807 (1968).

[12] B. R. A. Nijboer and F. W. de Wette, Physics **23**, 309 (1957).

This can be compared with the experimental result

$$D(\text{expt}) = 7.65\times 10^{-4}\ \text{cm}^{-1} \tag{15}$$

due to Feher.[6]

Though the total point-charge contribution to D agrees in sign with the experimental result, it is an order of magnitude less. The BO contribution is dominant and is of the same sign as the experimental result. If we compare the total spin-spin contribution and the experimental result, the former is two orders of magnitude less than the latter and is opposite in sign. It is worth noting that $D_{SS}(d\rightarrow s)$ is an order of magnitude less than $D_{SS}(d\rightarrow d)$, and about half of $D_{SS}(d\rightarrow g)$. The contributions from D_{ODS} and D_{WC} are negligibly small.

The reason for the point-charge contribution to D being an order of magnitude smaller than the experimental result is that $(B_4^0)'$ is very sensitive to the local distortion of the crystal in the neighborhood of the paramagnetic ion. $(B_4^0)'$ is mentioned because it is involved in the computation of D_{BO} [Eqs. (4) and (13)], which is the dominant contribution. $(B_4^0)'$ has been estimated without taking into account the local distortion due to the lattice relaxation in the presence of the impurity. However, if one calculates $(B_4^0)'$ (and other crystal-field components) after allowing for the lattice relaxation and thereby taking local distortion around the impurity ion into account, the theoretical results may be improved.

Now, the case of a uniaxial stress along [110] direction may be considered to estimate E. If the applied stress is represented by X', the dimensions of the distorted unit cell by a'', b'', c'', it can be shown that

$$a''=a(1+e_{xx})=a(1+e_{yy})=b'',$$
$$c''=a(1+e_{zz}), \tag{16}$$

where

$$e_{xx}=e_{yy}=\frac{X'}{2[c_{11}+c_{12}-2(c_{12}^2/c_{11})]},$$
$$e_{zz}=-\frac{c_{12}}{c_{11}}\frac{X'}{[c_{11}+c_{12}-2(c_{12}^2/c_{11})]}, \tag{17}$$

and the angle $2p$ between the X and Y axes of the crystal is given by

$$\cos 2p = X'/2c_{44}. \tag{18}$$

The angle $2p$ is $\pi/2$ before the application of the stress, as is clear from (18), since, when $X'\rightarrow 0$, $2p=\pi/2$. The quantities c_{11}, c_{12}, and c_{44} in (17) and (18) are elastic stiffness coefficients, which for MgO lattice have the values[10] given by (6) and

$$c_{44}=14.99\times 10^{11}\ \text{dyn/cm}^2. \tag{19}$$

For $X'=600$ kg/cm² the strain coefficients e_{xx}, e_{yy}, and e_{zz}, and $\cos 2p$ assume the values

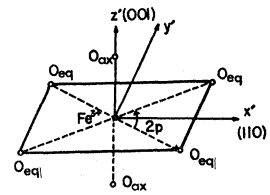

FIG. 3. Positions of the nearest-neighbor O^{2-} ions around Fe^{3+} ion for stress along [110] direction, and the disposition of x', y', and z' axes.

$$e_{xx}=e_{yy}=0.887787\times 10^{-4},$$
$$e_{zz}=-0.510313\times 10^{-4},$$
$$\cos 2p=0.196331\times 10^{-3}. \tag{20}$$

Now, the following expressions for the crystal fields B_4^2 and B_2^2, in units of $e^2/2a_0^5$ and $e^2/2a_0^3$, respectively, may be used:

$$B_4^2=\tfrac{1}{2}(\sqrt{10})\sum_j q_j[\sin^2\Theta_j(7\cos^2\Theta_j-1)\cos(2\Phi_j)]/R_j^5,$$
$$B_2^2=(\sqrt{3}/\sqrt{2})\sum_j q_j[\sin^2\Theta_j\cos(2\Phi_j)]/R_j^3, \tag{21}$$

where R_j is in units of a_0. The summation for j runs over all the external point charges $q_j\,|\,e\,|$ (constituting the distorted lattice) situated at (R_j, Θ_j, Φ_j) with respect to an origin taken at the site of the paramagnetic ion. The expressions (21) were evaluated employing the direct lattice summation method as described earlier. The values are

$$B_4^2=0.5143\times 10^{-5},$$
$$B_2^2=-3.1487\times 10^{-5}, \tag{22}$$

in units of $e^2/2a_0^5$ and $e^2/2a_0^3$, respectively. These results have also been checked with the help of the method due to Nijboer and de Wette.[12] It should be noted that the values B_l^m in (22) correspond to the axes system (x', y', z'), where the x' and z' axes are taken along [110] and [001] crystal directions of the distorted lattice, respectively, with y' being properly defined to correspond to the right-handed system (Fig. 3). B_4^2 and B_2^2 have been computed in the (x', y', z') axis system simply because the experimental results with which we shall compare also correspond to this axis system.

Substituting the values of B_4^2 and B_2^2 in the expressions for E [Eq. (4)], we get, in units of 10^{-4} cm^{-1},

$$E_{BO}=-0.909,$$
$$E_{SS}(d\rightarrow s)=+0.004,$$
$$E_{SS}(d\rightarrow d)=+0.002,$$
$$E_{SS}(d\rightarrow g)=+0.008,$$
$$E_{SS}(\text{total})=+0.014. \tag{23}$$

Combining these, one has

$$E(\text{point-charge}) = -0.90\times 10^{-4}\ \text{cm}^{-1}, \qquad (24)$$

which is in reasonable agreement with the experiment result

$$E(\text{expt}) = -1.62\times 10^{-4}\ \text{cm}^{-1}, \qquad (25)$$

due to Feher.[6]

It is interesting to notice that the BO contribution is again the dominant mechanism. It has the same sign as the experimental result and is more than 50% larger in magnitude. On the other hand, the spin-spin contribution is opposite in sign and two orders of magnitude less than the experimental result.

One may wonder why reasonable agreement with experimental results can be obtained for E but not for D. To clarify this point, one may compare the dominant parts of D_{BO} and E_{BO}. The expressions for D_{BO} and E_{BO} [Eq. (4)] depend on the crystal-field components $(B_4^0)'$ and B_4^2, respectively. The crystal field $(B_4^0)'$ is the difference of two large and nearly equal quantities $(B_4^0)_{\text{nc}}$ and $(14/5)^{1/2}(B_4^4)_{\text{nc}}$, while this is not true in case of B_4^2. The result is that $(B_4^0)'$ (but not B_4^2) is very sensitive to the local distortion of the lattice around the impurity ion. If one takes into account the distortion of the lattice due to lattice relaxation around the impurity, one expects to estimate a realistic value of $(B_4^0)'$ and thereby obtain a better result for D. Such a calculation for B_4^2 is also expected to give better agreement with experiment for E. Since lattice-relaxation calculations have not yet been made in this crystal, a simplified model, which assumes that the distortion around the impurity ion is the same as in the pure lattice, has been chosen.

III. OVERLAP CONTRIBUTIONS TO D AND E

In terms of the overlap and other two-center integrals, and the pertinent charge-transfer parameters, the expressions for D and E have been derived in II. These expressions are listed in Appendix B for convenience. Since the charge-transfer parameters are not known, one is forced to neglect them and compute the contributions which arise from the overlap alone to D and E.

In Fig. 2, the six nearest neighbors of Fe^{3+} are shown when the stress is applied along [001] direction. The O^{2-} ions along the direction of the stress are referred to as O_{ax} while those on the equatorial plane as O_{eq}. The oxygen ions O_{eq} lie on the vertices of a square with Fe^{3+} at the center. The distance of the oxygen ions O_{ax} from Fe^{3+} is $c'/2$, while that of O_{eq} from Fe^{3+} is $a'/2$, where c' and a' are given by (7) and (9). Since the angle between the diagonals of the square in the equatorial plane is $\pi/2$, the spin Hamiltonian parameter E vanishes in this case [see Eqs. (B12), (B13), (B14), (B23)–(B26)]. If the two distances Fe^{3+}–O_{ax} and Fe^{3+}–O_{eq} are equal, the overlap and other two-center integrals corresponding to these distances become equal and consequently D vanishes. However, if the distances Fe^{3+}–O_{ax} and Fe^{3+}–O_{eq} are unequal, D is nonzero. This is clear from Eqs. (B1), (B2), (B7), (B8), (B11), (B15)–(B18), and (B21).

One can evaluate D starting from the expressions (B1), (B2), (B7), (B8), (B11), (B15)–(B18), (B21) and the relevant expressions for local, nonlocal, and distant contributions arising from spin-spin and spin-orbit mechanisms. To this end, one needs to calculate five types of integrals, namely, $S_i(\text{O}_j)$, $g_{d,i}^{n,m}(\text{O}_j i)$, $h_{d,i}^{n,m}(\text{O}_j i)$, $\zeta_{d,2}(\text{O}_j i)$, and $\zeta_{p,p}$ as expressed by (B5), (B9), (B10), (B19), and (B22), respectively. The integrals $S_i(\text{O}_j)$, $g_{d,i}^{n,m}(\text{O}_j i)$, $h_{d,i}^{n,m}(\text{O}_j i)$, and $\zeta_{d,2}(\text{O}_j i)$ arise from the two-center matrix elements between orbitals of Fe^{3+} and O^{2-}. $S_i(\text{O}_j)$ are the overlap integrals between $3d$ orbitals of Fe^{3+} and $2s$ and $2p$ orbitals of O^{2-} ions. Here, j refers to the particular neighbor and i to the $2s$, $2p_\sigma$ and $2p_\pi$ orbitals with $(L=0, M=0)$, $(L=1, M=0)$, and $(L=1, M=\pm 1)$, respectively. In the same notation, the quantities $g_{d,i}^{n,m}(\text{O}_j i)$ and $h_{d,i}^{n,m}(\text{O}_j i)$ are the two-center double integrals between $3d$ orbitals of Fe^{3+} and $2s$, $2p_\sigma$, and $2p_\pi$ orbitals of the oxygen ion O_j. The integral $\zeta_{d,2}(\text{O}_j i)$ arises from the matrix elements of the spin-orbit operator $\zeta(r)$ [Eq. (B20)] between $3d$ orbitals of Fe^{3+} and $2s$, $2p_\sigma$, and $2p_\pi$ orbitals of the oxygen ion denoted by O_j. The quantity $\zeta_{p,p}$ [Eq. (B22)] is the conventional spin-orbit coupling constant for O^{2-}. For calculating $\zeta_{p,p}$ one requires the spin-orbit operator $\zeta(r)$ which refers to the oxygen nucleus. This operator, defined in Eq. (B20), can be obtained from the potential $V(r)$ given by

$$V(r) = (1/u_{2p}^0)(d^2u_{2p}^0/dr^2) - (2/r^2). \qquad (26)$$

In Eq. (26), u_{2p}^0 is r times the normalized $2p$ radial wave function for O^{2-}.

Similarly, for the integrals $\zeta_{d,2}(\text{O}_j i)$ one is concerned with the spin-orbit operator $\zeta(r)$ on the Fe^{3+} ion, and therefore

$$V(r) = (1/u_d^0)(d^2u_d^0/dr^2) - (6/r^2) \qquad (27)$$

can be used. The functions $\alpha_l(\text{O}_j LM \mid a_j r)$ needed for $S_i(\text{O}_j)$, $g_{d,i}^{n,m}(\text{O}_j, i)$, $h_{d,i}^{n,m}(\text{O}_j i)$, and $\zeta_{d,l}(\text{O}_j i)$ are the radial parts in the expansion of the wave functions for oxygen about Fe^{3+} as a center. Explicitly, it is defined as

$$\Phi(\text{O}LM \mid R\Theta\Phi) = \sum_{l=0}^{\infty} r^{-1}\alpha(\text{O}LM \mid ar)Y_l^M(\theta, \phi), \qquad (28)$$

where (R, Θ, Φ) are the polar coordinates of a point with respect to the oxygen ion O, the polar axis being taken as the line joining Fe^{3+} and the oxygen ion O under consideration; (r, θ, ϕ) represent the polar coordinates with the same polar axis but Fe^{3+} as origin. For a general form of the α function and its evaluation one may consult II. The derivation of the general form has been given elsewhere.[13]

[13] R. R. Sharma, J. Math. Phys. 9, 505 (1968).

TABLE III. Table of overlap and two-center spin-orbit integrals for stress along [001] direction.

j	$S_s(O_j)$	$S_\sigma(O_j)$	$S_\pi(O_j)$	$\zeta_{d,2}(O_js)$	$\zeta_{d,2}(O_j\sigma)$	$\zeta_{d,2}(O_j\pi)$
eq	−0.037392	−0.057666	0.036594	−0.323993	−0.838693	0.437913
ax	−0.037345	−0.057631	0.036556	−0.323504	−0.838284	0.436702

As regards the choice of the wave function for O^{2-} employed for the calculation, we use $2p$ wave function as used by Yamashita and Kojima[14] in their calculation on MgO. This wave function is expressed as the sum of two exponentials given by

$$u_{2p}^0 = 6.872r^2(e^{-2.9r} + 0.15e^{-1.1r}). \tag{29}$$

The $2s$ wave functions for O^{2-} are not available to this time and therefore the $2s$ Hartree-Fock wave function (as calculated by Hartree, Hartree, and Swirles[15]) for O^- has been used. There will be some variation in the radial wave function in going from O^- to O^{2-}. However, this variation is expected to cause only a small change in the final overlap contributions to D and E from the $2s$ orbital relative to the dominating contribution from the $2p$ orbital.

Utilizing these wave functions, one can calculate the integrals $S_i(O_j)$, $g_{d,l}^{n,m}(O_ji)$, $h_{d,l}^{n,m}(O_ji)$, $\zeta_{d,2}(O_ji)$, and $\zeta_{p,p}$. The values of the integrals $S_i(O_j)$ and $\zeta_{d,2}(O_ji)$ are listed in Table III. The integrals $g_{d,l}^{n,m}(O_{eq}i)$ and $h_{d,l}^{n,m}(O_{eq}i)$ are presented in Table IV, and $g_{d,l}^{n,m}(O_{ax}i)$ and $h_{d,l}^{n,m}(O_{ax}i)$ are given in Table V. The calculated value of $\zeta_{p,p}$ is found to be 67 cm^{-1}. It is worth remarking here that if $\zeta_{d,d}$, the spin-orbit coupling constant for $3d$ electron of Fe^{3+}, defined by

$$\zeta_{d,d} = \langle u_d^0 \mid \zeta(r) u_d^0 \rangle,$$

is evaluated using Eqs. (B20) and (27), we obtain $\zeta_{d,d} = 397.13$ cm^{-1}. The calculated value of $\zeta_{d,d}$ is thus close to the value of $\zeta = 400$ cm^{-1} used in Sec. II. The same value (400 cm^{-1}) for the coupling constant shall be used in this section for evaluating overlap contributions. Knowing the required integrals the local, nonlocal, and distant contributions to D which are listed in Table VI have been estimated. Thus, the combined overlap contribution is

$$D(\text{overlap}) = -0.05 \times 10^{-4}\ \text{cm}^{-1}, \tag{30}$$

which is opposite in sign and two orders of magnitude less than the experimental result [Eq. (15)]. It is also opposite in sign and an order of magnitude less than the point-charge contribution [Eq. (14)].

For the evaluation of the parameter E due to overlap, the procedure used is identical to that used for D. For uniaxial stress along the [110] direction, the nearest-neighbor environment is shown in Fig. 3. In this case the distances Fe^{3+}–O_{eq} and Fe^{3+}–O_{ax} are given by $a''/2$ and $c''/2$, respectively, where a'' and c'' can be obtained from (16) and (20). The angle subtended by adjacent O_{eq} ions at Fe^{3+} (Fig. 3) is $2p$, which is defined by (18) and (20). One can now use the expressions (B12)–(B14) and (B23)–(B26) in order to estimate local, nonlocal, and distant contributions to E. However, these expressions require the values of the overlap and other two-center integrals corresponding to the distance Fe^{3+}–O_{eq}. Since the parameter E is sensitive to $\cos 2p$ and is relatively independent of the small difference between Fe^{3+}–O_{eq} and $a/2$, we can set $r(Fe^{3+}\text{–}O_{eq}) \simeq r(Fe^{3+}\text{–}O_{ax}) \simeq a/2$ when calculating the overlap and two-center integrals. This situation is quite different from the situation for D where the difference between the two distances Fe^{3+}–O_{eq} and Fe^{3+}–O_{ax} is responsible

TABLE IV. The quantities $g_{d,l}^{n,n+3}(O_{eq}i)$ and $h_{d,l}^{n,n+3}(O_{eq}i)$ for stress along [001] direction. Integrals not required are not given.

l, i	$g_{d,l}^{0,3}(O_{eq}i)$	$h_{d,l}^{0,3}(O_{eq}i)$	$g_{d,l}^{2,5}(O_{eq}i)$	$h_{d,l}^{2,5}(O_{eq}i)$	$h_{d,l}^{4,7}(O_{eq}i)$
0, s	···	−0.011264	−0.003553	···	···
2, s	−0.000856	−0.004535	−0.000557	−0.001541	···
4, s	···	−0.001241	−0.000058	−0.000309	−0.000143
0, σ	···	−0.061568	−0.022582	···	···
2, σ	−0.002395	−0.010180	−0.001547	−0.003813	···
4, σ	···	−0.001704	−0.000140	−0.000491	−0.000249
2, π	0.001222	0.005480	0.000791	0.001998	···
4, π	···	0.001327	0.000078	0.000344	0.000163

[14] J. Yamashita and M. Kojima, J. Phys. Soc. Japan **7**, 261 (1952).
[15] D. R. Hartree, W. Hartree, and B. Swirles, Phil. Trans. Roy. Soc. London **A238**, 229 (1939).

TABLE V. The quantities $g_{d,l}{}^{n,n+3}(O_{ax}i)$ and $h_{d,l}{}^{n,n+3}(O_{ax}i)$ for stress along [001] direction. Integrals not required are not given.

l, i	$g_{d,l}{}^{0,3}(O_{ax}i)$	$h_{d,l}{}^{0,3}(O_{ax}i)$	$g_{d,l}{}^{2,5}(O_{ax}i)$	$h_{d,l}{}^{2,5}(O_{ax}i)$	$h_{d,l}{}^{4,7}(O_{ax}i)$
$0, s$	···	−0.011247	−0.003548	···	···
$2, s$	−0.000854	−0.004528	−0.000556	−0.001538	···
$4, s$	···	−0.001238	−0.000057	−0.000308	−0.000142
$0, \sigma$	···	−0.061513	−0.022560	···	···
$2, \sigma$	−0.002393	−0.010171	−0.001546	−0.003810	···
$4, \sigma$	···	−0.001692	−0.000128	−0.000483	−0.000242
$2, \pi$	0.001220	0.005474	0.000790	0.001995	···
$4, \pi$	···	0.001319	0.000047	0.000336	0.000155

for determining the value of D. In Table VII, the local, nonlocal, and distant contributions to E arising from spin-spin and spin-orbit interactions are listed. Combining the various contributions,

$$E(\text{overlap}) = 0.06\times 10^{-4}\ \text{cm}^{-1}, \tag{31}$$

which is about 27 times smaller than the experimental result [Eq. (25)] and also differs in sign. It also differs in sign from point-charge contribution [Eq. (24)] and is about 15 times smaller in magnitude.

IV. RESULTS AND DISCUSSION

In the case of $MgO:Fe^{3+}$, the estimates of the point-charge and overlap contributions to (i) D for the stress along the [001] direction and (ii) E for the stress along the [110] direction have been made and these are sufficient to determine the two independent spin-lattice constants C_{11} and C_{44} with the help of the relations given in Sec. I. The expressions (14), (24), (30), and (31) for D and E correspond to the following point-charge and overlap contributions to C_{11} and C_{44} (in units of 10^{-13} cm/dyn):

$$\begin{aligned} C_{11}(\text{point-charge}) &= +2.11,\\ C_{44}(\text{point-charge}) &= -3.06,\\ C_{11}(\text{overlap}) &= -0.15,\\ C_{44}(\text{overlap}) &= +0.21. \end{aligned} \tag{32}$$

These are comparable to the experimental results[6] (in units of 10^{-13} cm/dyn) of

$$\begin{aligned} C_{11}(\text{expt}) &= +26,\\ C_{44}(\text{expt}) &= -5.5. \end{aligned} \tag{33}$$

TABLE VI. Various contributions to D in units of 10^{-4} cm^{-1}.

Mechanism	Local	Nonlocal	Distant	Total
Spin–spin	0.027	−0.111	···	−0.084
Spin–orbit	0.047	−0.003	−0.009	+0.035
Total				−0.049

It is interesting to note that the point-charge contributions [Eqs. (32)] predict the same sign of C_{11} and C_{44} as experiments [Eq. (33)]. However, while the point-charge contribution to C_{11} is about an order of magnitude less than the experimental value, the point-charge contribution to C_{44} is in reasonable agreement with experiment. The overlap contributions to C_{11} and C_{44} are opposite in sign and about 160 and 27 times, respectively, smaller than the corresponding experimental values. Therefore, the effect of overlap cannot improve the point-charge results for C_{11} and C_{44}. One might be tempted to attribute this to the neglect of charge transfer covalency. However, it is evident from the expressions (Appendix B) for D and E due to overlap and charge-transfer effects that a reasonable amount of charge-transfer covalency cannot improve the results.

The present overlap contributions to C_{11} and C_{44} are much less than the experimental results. This is in contrast with Kondo's conclusions.[16] Kondo[16] computed overlap contributions for Mn^{2+} in MgO by fitting his formula to the observed experimental results and determined a reasonable magnitude of the overlap parameter for σ-type binding neglecting charge-transfer covalency. This led him to conclude that the overlap mechanism could account for the coupling constants. This is in contrast to the conclusion in the present study, where the detailed calculations considering local, nonlocal, and distant contributions show that the overlap contributions are much less than the experimental results and also differ in sign. The main reasons why the present conclusions differ from Kondo's are that he (i) considered only the local contributions to the spin-lattice

TABLE VII. Various contributions to E in units of 10^{-4} cm^{-1}.

Mechanism	Local	Nonlocal	Distant	Total
Spin–spin	0	0.059	···	0.059
Spin–orbit	0	0.001	0.003	0.004
Total				0.063

[16] J. Kondo, Progr. Theoret. Phys. (Kyoto) 28, 1026 (1962).

coupling constants arising from σ overlap alone, and (ii) approximated, as mentioned in II, the integrals $\zeta_{d,2}(O_j\sigma)$ by $\zeta_{d,d}S_\sigma(O_j)$, thereby making them about 20 times larger and giving large contributions to the coupling constants. These points have been discussed in detail in II and therefore will not be elaborated here.

The reason why it has not been possible to predict a satisfactory value for C_{11} is that the actual displacement of the ions surrounding Fe^{3+} was not taken into account. This displacement of the ions is due to two effects, the first of which is the presence of the impurity. Not only does Fe^{3+} (which replaces Mg^{2+} at a lattice point) have a different ionic radius than Mg^{2+}, but it is also more positively charged by one unit than Mg^{2+}. Therefore, the external ions surrounding Fe^{3+} see the effect of this extra charge and move from their normal position into a different equilibrium position. This effect is most pronounced for the nearest-neighbor ions.

The second effect is due to the imposition of stress, which brings about further changes in the equilibrium position of the ions. In order to obtain the actual displacement of the ions, one must consider both of these effects simultaneously and allow the lattice to relax. The main contribution to C_{11} (or D) from point-charge model [Eq. (14)] is due to the BO mechanism [Eq. (13)], which depends on the unbalanced noncubic crystal field $(B_4^0)'$ [Eq. (10)]. The component $(B_4^0)'$ is zero for a cubic environment [see Eqs. (10) and (11)]. It is very sensitive to the immediate neighborhood of the impurity ion since it involves the difference of two large and nearly equal parts, viz., $(B_4^0)_{nc}$ and $\alpha(B_4^4)_{nc}$. If the actual displacement of the surrounding ions, after including lattice relaxation effects, is taken into account to calculate $(B_4^0)'$ (and also other required crystal fields) a good agreement between theory and experiment may be expected. Since the lattice relaxation calculations have not yet been made in this case, one has to choose a simplified model, viz., the displacement of the surrounding ions due to the stress is the same as in the pure lattice under the same stress.

It is possible to show that one can obtain a value of D (or C_{11}) close to the experimental value if the nearest-neighbor ions are displaced by a reasonable amount. This displacement is considered to arise both from the effect of the extra unit positive charge on Fe^{3+} compared to Mg^{2+} and from the size of Fe^{3+}. To begin with, consider that the stress along the [001] axis is present and that the effects of the extra charge on Fe^{3+} and of the size of Fe^{3+} are absent (see Fig. 2). Then, as we have seen in Sec. II, the ions O_{eq} are closer to Fe^{3+} than the ions O_{ax}. Now, impose the effect of the extra charge on Fe^{3+}. All the oxygen ions, each having two units of negative charge, are attracted by the extra charge on Fe^{3+}. But the O_{eq} ions, which are closer to Fe^{3+}, are influenced more than the O_{ax} ions. Consequently, the O_{eq} ions move farther toward the Fe^{3+} ion than the O_{ax} ions. The ions are not expected to move a large distance since the large size of Fe^{3+} prevents their motion. It is reasonable to assume that the O_{eq} ions are displaced towards the Fe^{3+} ion by 0.5% and the O_{ax} ions by 0.1% of their respective distances from the central ion in the presence of the applied stress. In this case the calculated values of the Blume–Orbach contribution to D comes out to be

$$D_{BO} = +8.06\times 10^{-4}\ \text{cm}^{-1}.$$

The same displacements of the nearest-neighbor ions change the value of D_{SS}(total) by about 5% and D_{ODS} and D_{WC} by much less than 1%. The combined contribution to D is thus nearly 8.06×10^{-4} cm^{-1}, which corresponds to the value $C_{11} = 27\times 10^{-13}$ cm/dyn. Thus, it may be seen that a slight and reasonable change in the position of the nearest-neighbor ions has brought a large enhancement in the value of C_{11}, and this brings the theoretical result closer to the experimental value [Eqs. (33)]. So, it is clear that the actual displacement of the ions surrounding Fe^{3+}, if considered in the calculation of the crystal fields, can explain the experimental result for D. On the other hand, the contributions to E, are sensitive to $\cos 2p$ and a small change (of the size mentioned above) in the position of the surrounding ions does not affect the value of E by more than 5%.

Since the Fe^{3+} ion has one positive charge more than Mg^{2+}, one is led to think that there will be a negative charge in the crystal to compensate for it. This negative charge will produce an additional axial field on the Fe^{3+} ion even in the absence of external stress. Since the terms D and E are found to be zero experimentally[6] in the spin Hamiltonian in the limit of vanishing external stress, it can be inferred that either the compensating charge is too far off to distort Fe^{3+} or its effect on D and E is undetectable within the limits of experimental error. Thus, the experimental values for D and E which have been interpreted are solely due to the external stress. Therefore, we cannot consider the effect of the compensating charge on the measured value of D and E.

The other defects, of minor importance in our treatment, are (1) the omission of quadrupolar contributions to crystal-field components, (2) inaccuracies in the one-electron wave functions, (3) the neglect of correlation effects, and (4) the deformation of the radial wave functions in the crystal under stress, especially for the loosely bound O^{2-}.

ACKNOWLEDGMENTS

The author is indebted to Professor T. P. Das for valuable discussions. Thanks are also due to Professor S. Sundaram and Dr. R. Luzzi for critically reading the manuscript.

APPENDIX A

The expressions derived in I for D and E for various mechanisms under the point-multipole approximation are listed here. The contributions to D and E from

the Blume-Orbach mechanism are given by the

$$D_{\mathrm{BO}}=(5^{1/2}/36)\langle r^4\rangle\zeta^2 p_{\alpha\gamma}(2p_{\alpha\alpha}-p_{\alpha\beta})(B_4^0)' \quad \text{(A1)}$$

and

$$E_{\mathrm{BO}}=-(\sqrt{2}/6)\langle r^4\rangle\zeta^2 p_{\alpha\gamma}(2p_{\alpha\alpha}-p_{\alpha\beta})B_4^2, \quad \text{(A2)}$$

where $\langle r^4\rangle$ is the expectation value of r^4 for a $3d$ electron of the paramagnetic ion (Fe^{3+}) under consideration, and ζ is the spin-orbit coupling constant for the electron of this ion. $(B_4^0)'$ and B_4^2 are the unbalanced axial noncubic and the fourth-order rhombic crystal fields, respectively. Explicitly, these are the coefficients in the potential terms

$$V_4=-(B_4^0)'(4\pi/9)^{1/2}\sum_i r_i^4 Y_4^0(i) \quad \text{(A3)}$$

and

$$V_4^2=-B_4^2(4\pi/9)^{1/2}\sum_i r_1^4[Y_4^2(i)+Y_4^{-2}(i)]. \quad \text{(A4)}$$

The quantities $p_{\alpha\alpha}$, $p_{\alpha\beta}$, and $p_{\alpha\gamma}$ in (A1) and (A2) are defined by

$$p_{\alpha\alpha}=\sum_{i=1}^{3}\frac{\alpha_i\alpha_i}{\Delta_i},$$

$$p_{\alpha\beta}=\sum_{i=1}^{3}\frac{\alpha_i\beta_i}{\Delta_i},$$

$$p_{\alpha\gamma}=\sum_{i=1}^{3}\frac{\alpha_i\gamma_i}{\Delta_i}, \quad \text{(A5)}$$

where α_i, β_i, and γ_i are the mixing parameters, and Δ_i are the eigenvalues obtained by diagonalizing the ${}^4\Gamma_4$ matrix in the presence of the cubic field.

As regards the contributions[17] to D and E arising from spin-spin mechanism we write

$$D_{\mathrm{SS}}=D_{\mathrm{SS}}(d\to s)+D_{\mathrm{SS}}(d\to d)+D_{\mathrm{SS}}(d\to g) \quad \text{(A6)}$$

with

$$D_{\mathrm{SS}}(d\to s)=-(g^2\beta^2B_2^0/20\sqrt{5}a_0^3)\times[3.57771h_{d\to s}^{0,3}-5.36656g_{d\to s}^{2,5}],$$

$$D_{\mathrm{SS}}(d\to d)=-(g^2\beta^2B_2^0/20\sqrt{5}a_0^3)[-1.27775g_{d\to d}^{0,3}+5.11101h_{d\to d}^{0,3}-2.19043(g_{d\to d}^{2,5}+h_{d\to d}^{2,5})],$$

$$D_{\mathrm{SS}}(d\to g)=-(g^2\beta^2B_2^0/20\sqrt{5}a_0^3)[9.19982h_{d\to g}^{0,3}-0.10952g_{d\to g}^{2,5}-5.47608h_{d\to g}^{2,5}-19.16629h_{d\to g}^{4,7}], \quad \text{(A7)}$$

and

$$E_{\mathrm{SS}}=E_{\mathrm{SS}}(d\to s)+E_{\mathrm{SS}}(d\to d)+E_{\mathrm{SS}}(d\to g) \quad \text{(A8)}$$

with

$$E_{\mathrm{SS}}(d\to s)=-(g^2\beta^2B_2^2/40\sqrt{5}a_0^3)\times[8.76356h_{d\to s}^{0,3}-13.1453g_{d\to s}^{2,5}],$$

$$E_{\mathrm{SS}}(d\to d)=-(g^2\beta^2B_2^2/40\sqrt{5}a_0^3)[-3.12984g_{d\to d}^{0,3}+12.51942h_{d\to d}^{0,3}-5.36544(g_{d\to d}^{2,5}+h_{d\to d}^{2,5})],$$

$$E_{\mathrm{SS}}(d\to g)=-(g^2\beta^2B_2^2/40\sqrt{5}a_0^3)[22.5349h_{d\to g}^{0,3}-0.26827g_{d\to g}^{2,5}-13.4136h_{d\to g}^{2,5}-46.9476h_{d\to g}^{4,7}]. \quad \text{(A9)}$$

The parameters B_2^0 and B_2^2 are the axial and rhombic crystalline fields occurring in the potential terms

$$V_2^0=-B_2^0(4\pi/5)^{1/2}\sum_i r_i^2 Y_2^0(i)$$

and

$$V_2^2=-B_2^2(4\pi/5)^{1/2}\sum_i r_i^2[Y_2^2(i)+Y_2^{-2}(i)]. \quad \text{(A10)}$$

The quantities $g_{d\to l}^{n,m}$ and $h_{d\to l}^{n,m}$ in (A7) and (A9) denote the integrals

$$g_{d\to l}^{n,m}=\int_0^\infty dr_1\frac{[u_d^0(1)]^2}{r_1^m}\int_0^{r_1}r_2^n u_d^0(2)u_{d\to l}^{(1)}(2)\,dr_2$$

and

$$h_{d\to l}^{n,m}=\int_0^\infty dr_2\frac{u_d^0(2)}{r_2^m}u_{d\to l}^{(1)}(2)\int_0^{r_2}r_1^n[u_d^0(1)]^2dr_1. \quad \text{(A11)}$$

In the above expressions, u_d^0 is r times the radial $3d$ wave function of the paramagnetic ion. The functions $u_{d\to l}^{(1)}$ ($l=s, d, g$) are the perturbations on u_d^0 due to the axial and rhombic potentials V_2^0 and V_2^2 and are the solutions of the differential equations

$$\left[-\frac{d^2}{dr^2}-\frac{6}{r^2}+\frac{1}{u_d^0}\left(\frac{d^2u_d^0}{dr^2}\right)\right]u_{d\to s}^{(1)}=r^2u_d^0,$$

$$\left[-\frac{d^2}{dr^2}+\frac{1}{u_d^0}\left(\frac{d^2u_d^0}{dr^2}\right)\right]u_{d\to d}^{(1)}=r^2u_d^0-\langle u_d^0\mid r^2\mid u_d^0\rangle u_d^0,$$

$$\left[-\frac{d^2}{dr^2}+\frac{14}{r^2}+\frac{1}{u_d^0}\left(\frac{d^2u_d^0}{dr^2}\right)\right]u_{d\to g}^{(1)}=r^2u_d^0. \quad \text{(A12)}$$

For the Orbach-Das-Sharma mechanism

$$D_{\mathrm{ODS}}=(B_2^0)^2(5^{1/2}/192\pi)[\zeta^2p_{\alpha\gamma}(2p_{\alpha\alpha}-p_{\alpha\beta})]\times(M_2-4M_1+3M_0), \quad \text{(A13)}$$

where

$$M_m=(8\pi/5)\sum_{l=0,2,4}a_{ml}\langle u_d^0\mid r^2\mid u_{d\to l}^{(1)}\rangle \quad \text{(A14)}$$

[17] The expressions (52) and (60) of I corresponding to the expressions (A7) and (A9) given here used the incorrect approximation $g_{d\to l}^{n,m}=h_{d\to l}^{n,m}=\frac{1}{2}f_{d\to l}^{n,m}$, where $f_{d\to l}^{n,m}$ is given by Eq. (48) of I for $k=2$. The corrected results for the cases considered in I eliminating this approximation have been given elsewhere [R. R. Sharma, T. P. Das, and R. Orbach, Phys. Rev. **171**, 378 (1968)].

with

$$\mathbf{a}=\begin{pmatrix} a_{20} & a_{22} & a_{24} \\ a_{10} & a_{12} & a_{14} \\ a_{00} & a_{02} & a_{04} \end{pmatrix}=\begin{pmatrix} 0 & 4/49 & 3/49 \\ 0 & 1/49 & 6/49 \\ 1/5 & 4/49 & 36/245 \end{pmatrix}. \tag{A15}$$

For the Wantanabe mechanism with cubic field,

$$D_{\mathrm{WC}}=-\tfrac{1}{70}(\langle r^2\rangle^2/\Delta_{DS})(B_2^0)^2[\zeta^2\,|\,p_{\alpha\alpha}+(4/7)p_{\alpha\beta}\,|^2], \tag{A16}$$

where Δ_{DS} is the energy of the ^4D state above the ^6S level.

APPENDIX B

In this Appendix, we list the expressions derived in II for D and E under the overlap and charge-transfer model. The local, nonlocal, and distant contributions arising from spin-spin and spin-orbit interactions are written down separately. All the expressions contain terms up to second order in overlap and charge-transfer covalency.

The local contribution to D from spin-spin interaction is given by

$$D_{\mathrm{SS}}{}^{\mathrm{l}}=D_{\mathrm{SS}}{}^{\mathrm{l}}(s)+D_{\mathrm{SS}}{}^{\mathrm{l}}(\sigma)+D_{\mathrm{SS}}{}^{\mathrm{l}}(\pi), \tag{B1}$$

where

$$D_{\mathrm{SS}}{}^{\mathrm{l}}(s)=(6D_0/7)\{[S_s{}^2(\mathrm{O_{ax}})-\gamma_s{}^2(\mathrm{O_{ax}})]-[S_s{}^2(\mathrm{O_{eq}})-\gamma_s{}^2(\mathrm{O_{eq}})]\}[f_{d,d}{}^{0,3}-(8/7)f_{d,d}{}^{2,5}]. \tag{B2}$$

The expression (B2) gives the contributions arising from overlap and charge-transfer effects of $2s$ wave functions of the ligand ions (O^{2-}). Here

$$D_0=-g^2\beta^2/20a_0{}^3, \tag{B3}$$

and $S_s(\mathrm{O_{ax}})$ and $\gamma_s(\mathrm{O_{ax}})$ are the overlap and charge-transfer covalency parameters for the ligand ion designated by $\mathrm{O_{ax}}$ (see Figs. 2 and 3). $S_s(\mathrm{O_{eq}})$ and $\gamma_s(\mathrm{O_{eq}})$ carry similar meanings. The symbol $f_{d,d}{}^{n,m}$ represents the integrals

$$f_{d,d}{}^{n,m}=\iint u_d{}^0(1)u_d{}^0(2)\times(r_<{}^n/r_>{}^m)u_d{}^0(1)u_d{}^0(2)\,dr_1dr_2. \tag{B4}$$

The expressions for $D_{\mathrm{SS}}{}^{\mathrm{l}}(\sigma)$ and $D_{\mathrm{SS}}{}^{\mathrm{l}}(\pi)$, the contributions arising from $2p_\sigma$ and $2p_\pi$ orbitals of the ligand ions, can be obtained from (B2) on replacing s by σ and π, respectively. The overlap parameters $S_i(\mathrm{O}_j)$ ($i=s,\sigma,\pi$; $j=$eq, ax) are the matrix elements

$$S_i(\mathrm{O}_j)=\langle u_d{}^0\,|\,\alpha_2(\mathrm{O}_jLM\,|\,a_jr)\rangle \tag{B5}$$

with s corresponding to $L=0$, $M=0$, σ to $L=1$, $M=0$ and π to $L=1$, $M=\pm1$, a_j being the distance between the central ion (Fe^{3+}) and the ligand ion designated by O_j. The symbol $\alpha_l(\mathrm{O}_jLM\,|\,a_jr)$ denotes the α functions mentioned in II. A derivation of a general expression for the α function is given elsewhere.[13]

The local contribution to E via spin-spin interaction has been shown to vanish exactly, so that

$$E_{\mathrm{SS}}{}^{\mathrm{l}}=0. \tag{B6}$$

As regards the nonlocal contribution[18] to D from spin-spin interaction, we write

$$D_{\mathrm{SS}}{}^{\mathrm{nl}}=D_{\mathrm{SS}}{}^{\mathrm{nl}}(s)+D_{\mathrm{SS}}{}^{\mathrm{nl}}(\sigma)+D_{\mathrm{SS}}{}^{\mathrm{nl}}(\pi) \tag{B7}$$

with

$$\begin{aligned} D_{\mathrm{SS}}{}^{\mathrm{nl}}(s)=-4D_0[&([S_s(\mathrm{O_{eq}})+\gamma_s(\mathrm{O_{eq}})]\\ &\times\{-1.7889h_{d,0}{}^{0,3}(\mathrm{O_{eq}}s)+2.6833g_{d,0}{}^{2,5}(\mathrm{O_{eq}}s)\\ &+0.2857g_{d,2}{}^{0,3}(\mathrm{O_{eq}}s)-1.1429h_{d,2}{}^{0,3}(\mathrm{O_{eq}}s)\\ &+0.4898[g_{d,2}{}^{2,5}(\mathrm{O_{eq}}s)+h_{d,2}{}^{2,5}(\mathrm{O_{eq}}s)]\\ &-1.5333h_{d,4}{}^{0,3}(\mathrm{O_{eq}}s)+0.0183g_{d,4}{}^{2,5}(\mathrm{O_{eq}}s)\\ &+0.9127h_{d,4}{}^{2,5}(\mathrm{O_{eq}}s)+3.1944h_{d,4}{}^{4,7}(\mathrm{O_{eq}}s)\})\\ &-(\mathrm{eq}\rightarrow\mathrm{ax})], \end{aligned} \tag{B8}$$

where $(\mathrm{eq}\rightarrow\mathrm{ax})$ represents all the terms contained in the preceding bracket ( ) with the replacement of eq by ax in the integrals $S_i(\mathrm{O_{eq}})$, $g_{d,l}{}^{n,m}(\mathrm{O_{eq}}i)$, and $h_{d,l}{}^{n,m}(\mathrm{O_{eq}}i)$. The integrals $g_{d,l}{}^{n,m}(\mathrm{O}_ji)$ and $h_{d,l}{}^{n,m}(\mathrm{O}_ji)$ are defined by

$$g_{d,l}{}^{n,m}(\mathrm{O}_ji)=\int_0^\infty dr_1\frac{[u_d{}^0(1)]^2}{r_1{}^m}\times\int_0^{r_1}u_d{}^0(2)r_2{}^n\alpha_l(\mathrm{O}_jLM\,|\,a_jr_2)\,dr_2 \tag{B9}$$

and

$$h_{d,l}{}^{n,m}(\mathrm{O}_ji)=\int_0^\infty dr_2\frac{u_d{}^0(2)}{r_2{}^m}\alpha_l(\mathrm{O}_jLM\,|\,a_jr_2)\times\int_0^{r_2}[u_d{}^0(1)]^2r_1{}^n dr_1 \tag{B10}$$

with

$$i=s(L=0,\,M=0),\qquad \sigma(L=1,\,M=0),$$
$$\pi(L=1,\,M=\pm1);\qquad j=\mathrm{eq,\ ax}.$$

The expression for $D_{\mathrm{SS}}{}^{\mathrm{nl}}(\sigma)$ can be obtained simply

[18] The expressions (58) and (69) of II corresponding to the expressions for $D_{\mathrm{SS}}{}^{nl}$ and $E_{\mathrm{SS}}{}^{nl}$ given here were based on the incorrect approximation

$$g_{d,l}{}^{n,m}(\mathrm{O}_ji)=h_{d,l}{}^{n,m}(\mathrm{O}_ji)=\tfrac{1}{2}f_{d,l}{}^{n,m}(0_jLM),$$

where $f_{d,l}{}^{n,m}(\mathrm{O}_jLM)$ is defined by Eq. (51) of II. The corrected results for the case considered in II without this approximation have been given elsewhere (Ref. 17).

by replacing s by π in (B8). As regards $D_{SS}^{nl}(\pi)$ we have

$$D_{SS}^{nl}(\pi)=-4D_0[([S_\pi(O_{eq})+\gamma_\pi(O_{eq})]\times\{0.2857g_{d,2}^{0,3}(O_{eq}\pi)-1.1429h_{d,2}^{0,3}(O_{eq}\pi)+0.4898[g_{d,2}^{2,5}(O_{eq}\pi)+h_{d,2}^{2,5}(O_{eq}\pi)]-2.7994h_{d,4}^{0,3}(O_{eq}\pi)+0.0333g_{d,4}^{2,5}(O_{eq}\pi)+1.6663h_{d,4}^{2,5}(O_{eq}\pi)+5.8321h_{d,4}^{4,7}(O_{eq}\pi)\})-(\text{eq}\rightarrow\text{ax})], \quad (B11)$$

where (eq→ax) represents the terms contained in the preceding bracket ( ) with the replacement of eq by ax.

It can be shown that the distant contribution via spin-spin interaction gives rise to terms of order higher than two in overlap and charge-transfer covalency parameters. Thus, up to second order in overlap and charge transfer, the distant contribution D_{SS}^{d} is zero.

The nonlocal contribution to E from spin-spin mechanism is

$$E_{SS}^{nl}=E_{SS}^{nl}(s)+E_{SS}^{nl}(\sigma)+E_{SS}^{nl}(\pi), \quad (B12)$$

where

$$E_{SS}^{nl}(s)=-4D_0\cos 2p[S_s(O_{eq})+\gamma_s(O_{eq})]\times\{5.3666h_{d,0}^{0,3}(O_{eq}s)-8.0498g_{d,0}^{2,5}(O_{eq}s)-0.8571g_{d,2}^{0,3}(O_{eq}s)+3.4286h_{d,2}^{0,3}(O_{eq}s)-1.4694[g_{d,2}^{2,5}(O_{eq}s)+h_{d,2}^{2,5}(O_{eq}s)]+4.5999h_{d,4}^{0,3}(O_{eq}s)-0.0548g_{d,4}^{2,5}(O_{eq}s)-2.7380h_{d,4}^{2,5}(O_{eq}s)-9.5831h_{d,4}^{4,7}(O_{eq}s)\}. \quad (B13)$$

For obtaining $E_{SS}^{nl}(\sigma)$ we simply replace s by σ in the above expression. For $E_{SS}^{nl}(\pi)$ we have

$$E_{SS}^{nl}(\pi)=-4D_0\cos 2p[S_\pi(O_{eq})+\gamma_\pi(O_{eq})]\times\{-0.8571g_{d,2}^{0,3}(O_{eq}\pi)+3.4286h_{d,2}^{0,3}(O_{eq}\pi)-1.4694[g_{d,2}^{2,5}(O_{eq}\pi)+h_{d,2}^{2,5}(O_{eq}\pi)]+8.3982h_{d,4}^{0,3}(O_{eq}\pi)-0.1000g_{d,4}^{2,5}(O_{eq}\pi)-4.9990h_{d,4}^{2,5}(O_{eq}\pi)-17.4964h_{d,4}^{4,7}(O_{eq}\pi)\}. \quad (B14)$$

It can also be seen that, up to second order in overlap and charge transfer, the distant contribution E_{SS}^{d} vanishes.

Now we list the local, nonlocal, and distant contributions to D and E arising from spin-orbit interaction. The local contribution to D is

$$D_{SO}^{l}=D_{SO}^{l}(s)+D_{SO}^{l}(\sigma)+D_{SO}^{l}(\pi), \quad (B15)$$

where

$$D_{SO}^{l}(s)=[(\zeta_{d,d})^2/10\Delta]\{[S_s^2(O_{eq})-\gamma_s^2(O_{eq})]-[S_s^2(O_{ax})-\gamma_s^2(O_{ax})]\}, \quad (B16)$$

where $\zeta_{d,d}$ is the spin-orbit coupling constant for the electron on the paramagnetic ion (Fe^{3+}), and Δ is the average energy denominator. The expressions for $D_{SO}^{l}(\sigma)$ and $D_{SO}^{l}(\pi)$ can be obtained from (B16) simply by replacing s by σ and π, respectively.

The nonlocal contributions to D via spin-orbit mechanism

$$D_{SO}^{nl}=D_{SO}^{nl}(s)+D_{SO}^{nl}(\sigma)+D_{SO}^{nl}(\pi) \quad (B17)$$

with

$$D_{SO}^{nl}(s)=-(\zeta_{d,d}/5\Delta)\{\zeta_{d,2}(O_{eq}s)[S_s(O_{eq})+\gamma_s(O_{eq})]-\zeta_{d,2}(O_{ax}s)[S_s(O_{ax})+\gamma_s(O_{ax})]\}, \quad (B18)$$

where

$$\zeta_{d,l}(O_j i)=\int u_d^0\zeta(r)\alpha_l(O_jLM\mid a_j r)\,dr \quad (B19)$$

with

$$\zeta(r)=(e^2\hbar^2/4m^2c^2a_0^3)r^{-1}[dV(r)/dr]. \quad (B20)$$

$V(r)$ in (B20) is the potential seen by the electron. The potential $V(r)$ and the distance r are in units of $e^2/2a_0$ and a_0, respectively. The quantities $D_{SO}^{nl}(\sigma)$ and $D_{SO}^{nl}(\pi)$ in (B17) can be obtained by putting σ and π for s in (B18), respectively. The distant contribution to D from the spin-orbit interaction is

$$D_{SO}^{d}=-(2/15\Delta)\zeta_{d,d}\zeta_{p,p}\{[\lambda_\pi^2(O_{eq})-\lambda_\pi^2(O_{ax})]-\sqrt{3}[\lambda_\sigma(O_{eq})\lambda_\pi(O_{eq})-\lambda_\sigma(O_{ax})\lambda_\pi(O_{ax})]\} \quad (B21)$$

with

$$\lambda_i(O_j)=S_i(O_j)+\gamma_i(O_j)$$

for $i=s,\sigma,\pi$; $j=$eq, ax. The parameter

$$\zeta_{p,p}=\langle u_{2p}^0\mid\zeta(r)\mid u_{2p}^0\rangle \quad (B22)$$

is the spin-orbit coupling constant for the $2p$ electron of the ligand ion (O^{2-}).

The local contribution to E from spin-orbit mechanism exactly vanishes:

$$E_{SO}^{l}=0. \quad (B23)$$

The nonlocal contribution to E from spin-orbit interaction is

$$E_{SO}^{nl}=E_{SO}^{nl}(s)+E_{SO}^{nl}(\sigma)+E_{SO}^{nl}(\pi), \quad (B24)$$

where

$$E_{SO}^{nl}(s)=\tfrac{3}{5}(\zeta_{d,d}/\Delta)(\cos 2p)\zeta_{d,2}(O_{eq}s)\times[S_s(O_{eq})+\gamma_s(O_{eq})] \quad (B25)$$

and $E_{SO}^{nl}(\sigma)$ and $E_{SO}^{nl}(\pi)$ are obtained from (B25) by substituting σ and π for s, respectively.

Lastly, the distant contribution to E via spin-orbit mechanism is

$$E_{SO}^{d}=(2\zeta_{d,d}/5\Delta)\zeta_{p,p}(\cos 2p)\{[S_\pi(O_{eq})+\gamma_\pi(O_{eq})]^2-\sqrt{3}[S_\pi(O_{eq})+\gamma_\pi(O_{eq})][S_\sigma(O_{eq})+\gamma_\sigma(O_{eq})]\}. \quad (B26)$$